EJTIR

Issue 19(2), 2019
pp. 116-141
ISSN: 1567-7141
http://tlo.tbm.tudelft.nl/ejtir

# Multichannel queueing behaviour in urban bicycle traffic

**Rafał Kucharski**[1]
Department of Transport Systems, Cracow University of Technology, Poland.

**Arkadiusz Drabicki**[2]
Department of Transport Systems, Cracow University of Technology, Poland.

**Klaudia Żyłka**
Master Student, Cracow University of Technology, Poland.

**Andrzej Szarata**[3]
Department of Transport Systems, Cracow University of Technology, Poland.

The objective of this paper is to propose a method to analyse and describe cyclists' behaviour at signalized intersections with specific focus on the multichannel (multi-lane) queue phenomenon. As we observed, cyclists form queues without a fixed-lane and FIFO discipline, for which the classical, car-oriented analytical approach becomes insufficient. Cyclists' multichannel queueing behaviour is common and characterized by substantial degree of variability, especially in case of shorter queues which emerge regularly at cycle crossings. Although cyclist behaviour has been widely studied by transportation research community, their queueing behaviour picture is still incomplete. Namely, there is no method addressed to analyse the full scope of these phenomena and to quantify their impact on the cyclist queue performance.
To bridge this gap, we introduce the technique to observe multichannel queues and report relevant observations, which we then complement with a methodological framework to analyse obtained results and provide a complete multichannel queue description. We video-record cyclists as they enqueue to one of multiple channels, form the queue and smoothly merge into a single lane again as the queue discharges. We apply the method to analyse results from a pilot study of 160 cyclists forming 50 queues in the city of Krakow, Poland. The proposed method allows us to analyse and quantify the observed queue performance and its characteristics: the number of channels, their emergence process, channel and queue lengths, discharge process with FIFO violations, starting and discharging times. Findings from pilot study reveal that both queue length and discharge times strongly depend on queue formation process.
The contribution of this paper is the method to describe multichannel cyclist queueing behaviour, enriching current picture of bicycle flow and cyclists' behaviour. Since the method has been developed on relatively short queues (up to 10 cyclists), findings included in this paper primarily refer to such queue sizes. Nonetheless, the method is formulated in a generic way, applicable also for longer bicycle queues. Possible practical implications are new estimates for queue lengths and discharge times - useful for bicycle infrastructure design and traffic engineering purposes.

***Keywords***: *traffic flow, bicycle traffic, signalized intersections, queueing behaviour, signal control.*

[1] A: ul. Warszawska 24, 31-155 Krakow, Poland E: rkucharski@pk.edu.pl
[2] A: ul. Warszawska 24, 31-155 Krakow, Poland E: adrabicki@pk.edu.pl
[3] A: ul. Warszawska 24, 31-155 Krakow, Poland E: aszarata@pk.edu.pl

# 1. Introduction

Cycling is an increasingly popular mode of transport in multiple countries across the world. Investment in cycling infrastructure and sociocultural changes induce a substantial modal shift towards non-motorized modes of transport. This might be observed especially in urban areas, where the shift towards cycling is deemed a desirable trend. Such shift is expected to provide a significant relief for congested road transport networks and facilitate the transition towards sustainable, emission-free transport systems.

This trend can be also observed in Poland, where we identified the phenomena addressed by this paper and conducted a pilot study. Nowadays, modern Polish society is increasingly aware of the need to make responsible mobility choices, and thus likely to use bicycles for everyday commuter trips (Nosal, 2015). Recent comprehensive travel study for the Greater Warsaw agglomeration area revealed an increase in modal share of bicycle trips from a mere 0.6% in 2010 up to 3.1% in 2015, and this figure still seems to be constantly rising these days (WBR, 2015).

This poses a major challenge for traffic engineering and transport planning policies, which were historically oriented towards motorized traffic in first place (Roess et al., 2011). The car-dominated urban transport planning is nowadays being reoriented towards the cyclists' perspective, which calls for a more complex approach to cycling traffic in terms of traffic engineering, as well as traffic control and management. To achieve this, a comprehensive understanding of cyclists' behaviour is needed - a research topic being less-explored than the motorised traffic, with (as we report in this paper) some phenomena still not yet fully addressed since the landmark study of (Taylor & Davis, 1999).

Cyclist behaviour, which we aim to investigate in this study, relates to the queueing behaviour at signalized bicycle crossings. We are particularly interested in the phenomenon of multichannel queuing behaviour, with main emphasis on queuing process and the resulting queue structure. Cyclists' queuing behaviour appears to be substantially different from car traffic queuing process. As described below, we routinely observe that on a single-lane, bi-directional cycleway cyclists tend to queue in multiple lanes. Since there is no fixed lane discipline, they are free to form multiple channels of different lengths, the so-called multichannel queues. They self-organize into informal lanes (channels) and seamlessly merge into single-lane traffic again as they discharge. This leads to a number of interesting and yet not fully reported phenomena, which are of not only theoretical significance, but also of practical importance for bicycle traffic analysis.

When cyclists queue in a single channel, they form a FIFO (first-in, first-out) queue of length roughly proportional to the queue size (i.e. number of cyclists). Presumably, the queue of the same size is significantly shorter if two or more channels are formed. In this work we aim to analyse various queue formations to see how much these can be reduced in length due to formation of multiple channels. While cyclists within a channel obey the FIFO discipline, overtaking and leap-frogging behaviour between multiple channels is possible and quite common. This might have important implications for queue discharge times which may be shorter for multichannel queues. Moreover, cyclists forming a second channel may violate the FIFO discipline and overtake those queuing in the first channel, as they might expect to gain by enqueueing into a separate channel. Furthermore, the queue emergence process and its properties are non-deterministic, which is of non-negligible importance in the description of bicycle queuing behaviour.

Our objective is to report on these phenomena in a wider extent, and to introduce an analytical framework to describe cyclist queuing behaviour based on empirical observations. As part of this study, we analysed video recordings of cyclists who approach traffic signals, form the queue, start at green light and merge into single lane again. These observations were then analysed with the method proposed in this paper. The presented findings presented are based on a small, but an in-depth pilot case study of 160 cyclists in the city of Krakow (Poland) who formed 50 queues.

Despite a limited sample size, we managed to reveal phenomena and findings that were not fully reported before.

The paper is organized as follows. After this introduction, we formulate the contribution below. Then we summarise the literature review in chapter 2 and propose method in chapter 3. Chapter 4 presents results from case study, and a summary of this research with conclusions is provided in chapter 5.

### *1.1 Contribution*

The main contribution of this paper is a generic method for analysing the multichannel queuing behaviour at signalized bicycle crossings. Specifically, we present the technique of multichannel queue observation and data collection for further analysis, and then we propose an analytical framework to obtain a complete picture of multichannel queuing process. The method allows to identify and describe key properties of this process: number of channels formed, queue formation process and enqueueing decisions; resultant channel lengths and queue lengths; cyclists' start time within the channel and resultant queue discharge time and order. We also emphasise the non-deterministic nature of these phenomena which especially holds true for shorter bicycle queues and has important implications for describing the bicycle queues' performance.

The proposed method may be applied for generic cyclists' queue observations to understand the scale and consequence of multichannel behaviour especially in terms of queue lengths and discharge times. Our objective is to provide an analytical framework, which could then enrich the bicycle flow models with more realistic and accurate representation of cyclist behaviour.

The side contribution of this paper is the first (to the best of our knowledge) such complete report on multichannel cyclist queuing phenomena, obtained with the proposed method. A certain limitation of this study can be attributed to the sample size of field observations, and obtained pilot results cannot be of full statistical relevance. Nevertheless, we managed to reveal important phenomena in cyclists' queue formation process and formulate an improved framework for their analysis, which was the main objective of this research. The proposed method can be used to conduct a study on a bigger sample, to make the results much more transferable and generalizable. This could be then used to provide statistically sound indications for traffic management strategies (at signalized cycle crossings) and bicycle infrastructure design guidelines.

## 2. Literature review

Road infrastructure is shared by various users (pedestrians, cyclists and car drivers) and comprises both dedicated space for each of them (i.e. footways, bikeways, roadways) as well as shared areas where conflicts arise (i.e. junctions, crossings, mixed-traffic). Conflicts arising between multiple streams of traffic can be handled either in spatial (multi-level crossings) or temporal dimension (traffic signal controls). Methods to control these processes are nowadays highly developed, ranging from optimized static control, through actuated control, up to intelligent traffic control in the wider transport network (Roess et al., 2011). Output of control actions relies mainly on accurate information about demand volumes (number of vehicles) and its structure (splitting rates at the intersections), but also on behavioural assumptions imposed by flow models (Treiber & Kesting, 2013).

In this sense, efficient traffic control strategies strongly depend on proper understanding of traffic dynamics and its underlying assumptions. Among others, this includes starting times, acceleration and deceleration rates of particular vehicles, and importantly the queue forming process (Viti & van Zuylen, 2004), with pedestrian and cyclist perspective lately gathering increasing research momentum: (Lachapelle & Cloutier, 2017) analysed signal timings from the cyclists' perspective, (Chen et al., 2018) described how the convenience, safety, and leisure drives the cyclists' route choices, (Halldórsdóttir et al., 2014; Ghanayim & Bekhor, 2018) analyzed cyclists' route-choice process, while (Faghih-Imani et al., 2017) analysed how urban forms influence the bicycle usage.

### *2.1 Cyclists' behaviour*

While elementary characteristics are well-known and thoroughly investigated for car traffic, they remain still much less explored in case of bicycle traffic (Portilla et al., 2016). (Liang et al., 2012) demonstrated that bicycle traffic flow is substantially different from car traffic flow and, as argued by (Twaddle et al., 2014), classic traffic flow theory cannot properly describe cyclists' dynamics (acceleration, deceleration, speed profiles), space occupation and behaviour. Cyclist behaviour is characterized by a considerably higher degree of complexity: cyclists are more independent from the general road traffic and their movement is principally the result of individual decisions, rather than driving regulations, road markings or organized traffic flows. Bicycle dynamics (and attainable speed) are not determined by the vehicle engine, but rather by cyclists stamina (Parkin & Rotheram, 2010), and thus more influenced by personal (user) characteristics and preferences (Figliozzi et al., 2013). (Goni-Ros et al., 2018) show how bicycle users vary from recreational cyclists, elderly and children to professional bikers. Some of them might tend to travel in a more relaxed manner, and do not necessarily follow one another in a single-line manner, but often ride in interdependent groups. On top of that, cycling perceptions and attitudes strongly vary depending on local culture and case-specific conditions (Pojani et al., 2017).

Cyclist behaviour often exposes a significantly stochastic nature, and crucially, there is no strict lane discipline for cyclists. When forming a queue, they can stop in any position: a) behind the predecessor (by either keeping a distance or overlapping and forming a denser queue) or b) next to the predecessor, more interesting from research point of view, by creating a new channel. Such cycle lanes are created ad-hoc by arriving cyclists, who are free to choose their stopping position. Cycling flows tend to form irregular lanes and it may be hard to uniquely assign cyclist to a particular lane. This all amounts to a fairly complex system, much less-organized than the motorized traffic. Consequently, observing bicycle traffic is a more challenging task than observing car (vehicular) traffic.

### *2.2 Data collection*

Different data collection methods have been utilized to gather field observations of bicycle flow performance. Recent technological advancements enable even more sophisticated data collection techniques, facilitating analysis of cyclists' behaviour and its specific characteristics which cannot be easily traced with traditional methods. Bicycle traffic volumes can be nowadays measured, with quite reliable accuracy, by a wide range of detection devices induction loops, infrared sensors, pneumatic tubes and microwave sensors (Minge et al., 2017). GPS based big data is also a promising solution, thanks to the rising data availability (smartphone penetration rate etc.) and its applicability for various purposes of bicycle traffic research deriving behavioural patterns, forecasting network conditions etc. (Romanillos et al., 2016). Furthermore, increasing popularity of public bike rental schemes and e-bicycles also offers new (and important) possibilities for collecting bicycle big data and examining everyday bicycle usage patterns in urban areas, as noted by e.g. (X. Zhou, 2015), (Dozza et al., 2016). However, despite significant improvements in data collection techniques, key challenges remain with respect to data processing and especially the visual data interpretation. This topic has been recently gaining momentum both in academic and industrial research, with studies showing the increasing prospects of automated video recognition in analysis of cyclist behaviour ((Osowski, 2017), (Gon˜i-Ros et al., 2018)). Recent developments in automated video collection methods (Zangenehpour et al., 2015; Zangenehpour et al., 2016; Beitel et al., 2017) allow for an automated detection and analysis of different traffic user categories - cyclists, pedestrians, motorised traffic - within a relatively high degree of precision and reliability. Unfortunately, those methods might not always be applicable in state-of-the-practice, and still in many cases manual data processing might be necessary (at least at certain stages), which inhibits the scope of analysing bigger datasets and complex field observations.

### 2.3 *Bicycle flow descriptions*

Bicycle flow models, both mesoscopic and microscopic, have been developed and proposed by various authors, with an objective of capturing the difference between car traffic and bicycle traffic flow by accounting for the complexity of the bicycle movements and cyclists decision-making process. We refer here especially to the Cellular Automata (CA) (Nagel & Schreckenberg, 1992) and Social Force Models (SFM) (Liang et al., 2012), which form the basis for a substantial share of state-of-the-art bicycle flow models. These models address important features of bicycle traffic such as: the continuity of longitudinal and lateral cyclist movements; attractive-repulsive and psychological-physical driving forces (resulting from interactions with other users, obstacles, infrastructure objects); lane-changing discipline (Shen et al., 2011; Gould & Karner, 2009), distinct cycling regimes (acceleration, cruising, deceleration profiles) (Ma & Luo, 2016), hydrodynamic flow theory models (Li et al., 2014), to name just a few. (Twaddle et al., 2014) conclude that although cyclists' physics can be reasonably replicated in the state-of-the-practice bicycle models, cyclists' strategic behaviour remains much less covered, and a more detailed approach should not only model how cyclists navigate their route and progress through the network (i.e. how they behave), but also capture the reasoning behind their choices and interactions (i.e. why they behave so). (Twaddle et al., 2014; Gould & Karner, 2009) conclude that a more solid explanation of cyclists' behaviour is missing due to lack of accurate empirical data, and stated and observed preference, which consequently inhibits the development of more nuanced behavioural models.

At the time when the state-of-the-art research on bicycle traffic was summarized in the benchmark study of (Taylor & Davis, 1999), main research gaps at that time were indicated as: gap acceptance, interaction with other users in mixed-traffic, handling obstacles, and general design guidelines. Up to now many of these were covered, and findings relevant to the queueing behaviour at signalized intersections were also reported in research sources.

As summarized in (Taylor & Davis, 1999), first major findings in this respect concerned the capacity and LoS calculation guidelines for bicycle ways by (Miller & Ramey, 1975), extended then further to account for riding comfort and lateral-movement freedom by (Navin, 1994), examine the fundamental diagram interdependencies of bicycle traffic (i.e. relationship between speed, volume and density) (Botma & Papendrecht, 1991), and to include hindrance imposed by others by (Botma, 1995). Notably, (Raksuntorn & Khan, 2003) estimated the queue length growth rate of 1.2-1.3m per cyclist, and the lateral distance between cyclists queuing in parallel from 0.42 to 1.47m (with a mean value of 0.72m) per cyclist.

A certain number of researchers addressed bicycle dynamics at the intersections, for instance mean speed and its distribution, acceleration and deceleration, gap and lag acceptance. Sample results and detailed references can be found in (Taylor & Davis, 1999; Haifeng et al., 2013; Ling & Wu, 2004). (Ma & Luo, 2016) utilise a data-driven approach and distinguish three principal cycling regimes (acceleration, cruising at desired speed and deceleration). (Figliozzi et al., 2013) develop the methodology to estimate cyclists' acceleration and cruising speed distributions at signalized intersections, applicable for signal timing purposes and more suitable for case-specific conditions. The study notes that derived speed and acceleration profiles can be used to classify the bicycle group users, as demographics have a substantial impact upon resultant bicycle traffic dynamics. (Deng & Xu, 2014) indicate important aspects related to flow-density relationship of bicycle traffic at intersections, defining the longitudinal expansion of bicycle queue as a function of crossing width-to-length ratio. They stress the fact that maximum flow density does not occur at the crossing line, but takes place shortly after the discharge time which can be explained by the back-row cyclists moving faster than (or catching up with) the front-row cyclists. (Cao et al., 2011) derive linear regression models applicable for calculating queue lengths and densities as a function of the number of approaching cyclists. Interestingly, they observe that a piece-wise regression curve is more fitted to explain the N-shaped relationship between the rising queue length and increasing number of cyclists.

### 2.4 *Capacity*

Significant variations can be observed in capacity estimations of bicycle lanes and cycleways reported in different sources, as underlined by e.g. (D. Zhou et al., 2015). Values of 2000 to 3500 cyclists per hour per 1.0-1.2m bicycle lane width seem to be the most common, yet substantially higher values can also be found in certain sources. (Twaddle et al., 2014) explains this variability as a consequence of multiple queues (channels) forming within a single bicycle lane (we use the term channel - while in research sources these can be alternatively denoted as sub-lanes, lanes or files). A channel can be formed thanks to higher lateral flexibility of cyclists and more limited influence of leading vehicles (i.e. preceding cyclists) as compared to the car traffic. Consequently, capacity is not merely a function of the number of lanes, but essentially a function of total effective cycleway width (D. Zhou et al., 2015). Usually, a simple linear correlation between the capacity rate and bicycle lane width is assumed, which may not actually be the case in certain conditions. (Raksuntorn & Khan, 2003) mention that the lateral (cross-sectional) usage of bicycle lane becomes more effective as its width increases, without providing specific values though. They propose to express saturation flow rate as a function of time headway and number of channels, equal to 1500 bicycles per one hour per one channel. (Botma & Papendrecht, 1991) estimate the capacity of a 2.50-metre wide cycleway to be much higher than the standardized, fixed guideline at that time of ca. 5000 bicycles per hour. The assumed definition implies a bicycle channel width of ca. 0.78m and capacity estimations yield values of around 6000-6400 bicycles/hr when derived from the flow-density curve but once accounting for non-uniform headway distribution among cyclists, these reach up to 9000 bicycles/hr.

To better explain these relations, (Wang et al., 2011) introduced the fluid dispersion approach to estimate the intersection capacity. They argue that bicycles follow a fluid-stream model rather than a single particle behaviour and often form bicycle platoons. The proposed fluid-pipe model consists of three regimes (queuing before the intersection, a widening dispersion zone through the intersection, and merging into a free-flow cycleway) represented with a 3D cylindrical model which can cover queue channels (by increasing the queue width). The model, although providing valuable insights on physics of bicycle flow, does not address the strategic behaviour and lacks an empirical support.

(Raksuntorn & Khan, 2003) extended the bicycle traffic flow model at intersections by including the phenomenon of multiple queues per lane. Their aim was to establish an evidence-based estimate of saturation flow rate and start-up lost time for cyclists. They observe that the time headway between consecutive bicycle departures gradually decreases from ca. 2.0 secs per cyclist after the green-signal onset, down to ca. 0.80 secs after the departure of the fifth cyclist in the queue, after which it remains constant which they assume to be the saturation headway rate. (Goni-Ros et al., 2018) further report on empirical observations of bicycle queues at intersections and their macroscopic characteristics. They focus specifically on shockwave patterns in queue discharging process, which is related to the non-uniform headway distribution among dispersing cyclists. Results from their analysis indicate that the first-order description traffic flow theory, despite its general consistence, do not cover internal stochasticity, leading often to non-optimum outflow (i.e. discharge) conditions of bicycle traffic.

### 2.5 *Research gap*

In a summary, despite the increasing momentum in bicycle traffic research in recent years, the full scope of certain phenomena has not yet been covered and explained in a comprehensive way. Studies report on important aspects of bicycle traffic flow and underline differences with the classical car traffic flow theory, but often fall short of a full explanation of underlying behavioural phenomena (and their causality). State-of-the art methods for analysing the bicycle queuing behaviour remain vague with respect to certain characteristics, especially the queue formation, evolution and discharging processes, often dealing with these aspects in a rather generalized way. Notably, a more solid link between the non-deterministic nature of these phenomena and bicycle flow parameters is often missing, and consequently the present-day methods might miss the non-trivial implications of these aspects for cyclist queue performance. It also remains unclear how the variability of multichannel queuing phenomena might be associated with individual cyclists' decisions, how it would in turn shape their own cycling performance (time delays etc.) and finally, how this could impact the overall bicycle queue efficiency.

To sum up, the multichannel queue formation pattern is a vital feature in cyclist behaviour analysis - seems yet to lack comprehensive methods in state-of-the-art research, which would allow to analyse the full scope of such phenomena and quantify their impact upon bicycle traffic flow performance. Investigation of these phenomena at a more disaggregate level, with specific emphasis on the evolution and discharging patterns and their probabilistic properties, is necessary to improve our understanding of bicycle flow patterns at signalized crossings and arising consequences. We aim to contribute towards overcoming this research gap and extend the already identified considerations on cyclist queuing behaviour in further chapters of this paper.

# 3. Method

To perform our analysis of multichannel cyclist queuing phenomena, we conducted field observations of cyclists who approach the stop line at a signalized cycle crossing, form the queues and drive off once traffic signal turns green. We studied a busy, signalized intersection in the city of Krakow (Poland) along a popular cycle route in Krakow connecting eastern residential districts with central part of the city. The high quality of the designated cycleway at the selected location (separated route, smooth and safe layout enabling fast ride) attracted reasonable bike flows (of up to 400 cyclists per hour in each direction), leading to some unprecedented and unrecognised situations. Cyclist flows at the location are large enough to cause queue build-ups (which were not observed before) and cyclist need to establish their queuing behaviour. The cycleway is used by regular cyclists whose behaviour is motivated by travel time savings, experienced enough to optimize queuing behaviour.

Observed cyclists use their dedicated inlet and wait at the traffic signal head before entering the ca. 25m long cycle crossing. The cycleway is 3m wide with no additional widening on the approaches (inlets), as depicted in Figure 2. We observed up to three parallel queue channels, which filled the cycleway width, and presumably the fourth channel could not be formed any further due to width constraints (this is comparable to cycle channels widths reported in (Raksuntorn & Khan, 2003)).

The cycleway is bi-directional and does not have designated lanes (markings) for opposite streams of movement, so that cyclists need to merge when crossing to avoid conflicts with oncoming cyclists from the opposite direction. Cycle flows are asymmetrical, i.e. the inbound flow (towards the city centre) is higher in the morning peak, while in the afternoon peak the outbound flow prevails. Nonetheless, the oncoming cyclists were always present and cyclists discharging from multichannel queues had to merge into a single lane. While this might have not been the case anymore if the flows were higher, for the magnitude of flows reported in the paper no such conflicts could have been observed. The effective green signal phase for the cycleway is around 17s during the total cycle time of 120s. All the observed queues managed to discharge fully during a single green-signal phase, so no residual queues were observed.

## 3.1 *Video recording*

To analyse the behaviour, we video-recorded cyclists as they approach traffic signals, form the queues before stopping, drive off at the green light and merge back into single flow. Observations were gathered for a single direction at this intersection only, i.e. westbound approach (towards the city centre) during the AM peak. Each video recording period coincided with the signal cycle (ca. 120s), starting at the beginning of red phase (to record the queue formation) and finishing at the end of the green phase (to record the discharge process). Video camera was placed at a location depicted in Figure 2, so that it would capture all the consecutive stages of cyclist behaviour, as shown on the sample frame in Figure 1. Shooting angle allowed to record the enqueue positions and distances from the stop line.

Unfortunately, there is no readily applicable method to process the footage automatically, so the recordings were examined manually. They were processed frame by frame to track the instants of specific (benchmark) events: arriving at the stop line, entering and exiting the cycle crossing. The frame per second (fps) rate of the footage allowed to obtain a high-quality precision, down to a tenth of a second. Specific time instants were clearly identifiable from the footage. Stopping and starting times were identified as the instances when cyclists' foot touches down and is lifted up from the ground respectively. The discharge time was defined as period until the moment when the front wheel of a bicycle crossed the opposite stop line.

Fixed camera position allowed to keep precision of ca. 0.5m while measuring distances. We approximated distances relative to the stop line using fixed reference points (lines, signs, curbs, etc.). Since identifying queuing cyclists' position may be ambiguous (e.g. due to bending the front wheel while stopping), the front axis position was used as the reference point. Assigning cyclists to channels was a relatively straightforward task, as discussed in the subsequent section. In general, the manual processing of video recordings, though time consuming, was rather straightforward, repetitive and did not result in any noticeable interpretation errors.

*Figure 1. Sample footage frame*

### *3.2 Data processing and formalisation*

From the raw footage, we intended to reproduce the cyclists' space-time trajectories:

$$x_i(\tau) \tag{1}$$

, where position $x$ of cyclist $i$ is recorded over time $\tau$. The time $\tau$ is measured relatively to green phase time and is equal zero at the instance when signal turns to green, with negative values for arrivals and positive values for start time and discharge time. We recorded cyclists' longitudinal position (relative to the stop line, negative before they cross the line and positive afterwards) as well as latitudinal position within the cycleway cross-section (relative to the right curb, increasing from right to left), as depicted in figure 3.

Though we recorded full cyclist trajectories, we processed the footage into specific space-time points only. We introduce following mappings of the raw trajectory into sets of specific points $\boldsymbol{x_i}$ of gradually increasing number of elements (eq. 2, 4 and 7). In the first place, we were interested in cyclists' arrival times (when and where they come to a stop), starting times (when they drive off and enter the crossing) and discharge times (when they cross the opposite stop line and exit the crossing). This yields the following map:

$$x_i(\tau) \rightarrow x_i = (t_a, x_a, y_a, x_m, t_s, t_d, t_m) \tag{2}$$

, where:

- $t_a$ is an arrival instance (relative to the green signal phase),
- $x_a$ and $y_a$ are latitudinal and longitudinal arrival positions respectively,
- $t_s$ is starting time,
- $t_d$ is discharge time,
- $x_m$ and $t_m$ are the position and time of merging back into the single channel again at the discharging.

The longitudinal position $x_a$ is measured as the position of the front wheel axis (usually when cyclist's front wheel is turned slightly to the side, and thus measuring the nearest point would be biased), with the 0.5m accuracy as described above.

Cyclists arriving during a red signal form a queue $\boldsymbol{Q}$, formally being the set of observed cyclists:

$$Q = \{x_1, x_2, ..., x_i, ..., x_n\} \tag{3}$$

Each cyclist in the queue is further assigned with his own index $i$, channel $n$ and channel position $j$. The indexes are assigned sequentially as cyclists arrive and are recalculated anew for every consecutive queue. Channels are assigned from the latitudinal position $y_a$, and channel positions are assigned sequentially within the channel. To identify the cyclists and channels more precisely, we first assumed that each channel has a leader (first cyclist) and further enqueueing cyclists may either enqueue into the already formed channel or form a new channel. We first labelled channels by looking at their leaders and then labelled each cyclist by looking at his predecessor. This way even if the channels were ambiguous from the footage, they were logically identifiable as a sequence. The channels are numbered similarly to traffic lanes i.e. from right to left.

Using the above notation, the mapping of (eq. 2) is further extended with the queue-related indexes into:

$$x_i(\tau) \rightarrow x_i = (t_a, x_a, y_a, x_m, t_s, t_d, t_m, n, j) \tag{4}$$

A queue can be decomposed into a set of channels, identified as a subset of cyclists queuing in a respective channel: $\boldsymbol{C_k} = \{\boldsymbol{x_i} \in \boldsymbol{Q} : n(\boldsymbol{x_i}) = k\}$.

For queues and channels the following can be further derived:

- size, i.e. number of cyclists in a channel or queue respectively: $\|C\|$, $\|Q\|$;
- length of channel $l(\boldsymbol{C})$ or queue $l(\boldsymbol{Q})$, i.e. a stop position of the furthest (last) cyclist;

- spatial distribution (ordered arrival positions): $(x_a(\mathbf{x_i}) : x_i \in \mathbf{Q})$;
- queue formation order, i.e. the sequence of chosen channels: $(n(\mathbf{x_i}) : \mathbf{x_i} \in \mathbf{Q})$;
- number of channels in the queue: $N(\mathbf{Q}) = max(n(\mathbf{x_i}) : \mathbf{x_i} \in \mathbf{Q})$;
- starting process, i.e. the sequence of consecutive starting times: $(t_s(\mathbf{x_i}) : \mathbf{x_i} \in \mathbf{Q})$;
- merging process, i.e. times and positions at which cyclists merge back into a single channel again: $(t_m(\mathbf{x_i}) : \mathbf{x_i} \in \mathbf{Q})$;
- discharge time, i.e. discharge time of the last cyclist: $t_d(\mathbf{Q}) = max(t_d(\mathbf{x_i}) : \mathbf{x_i} \in \mathbf{Q})$;
- discharge process: $(t_d(\mathbf{x_i}) : \mathbf{x_i}, \in \mathbf{Q})$;
- discharge order, i.e. sequence of cyclists ordered by increasing discharge times.

For the sake of brevity, we will use:

$$Q(i,n) \tag{5}$$

to denote the queue of *i* cyclists who formed *n* channels. This can be further extended to:

$$Q(i,n,\{a\,|\,b\,|\,c\}) \tag{6}$$

when the number of cyclists $\{a\,|\,b\,|\,c\}$ in respective channels is being referred to. Thanks to this, we can trace the queue evolution by recording the state of the queue at the arrival, which constitutes the final mapping:

$$x_i(\tau) \rightarrow x_i = (t_a, x_a, y_a, x_m, t_s, t_d, t_m, n, j, Q(i', n', \{a\,|\,b\,|\,c\})) \tag{7}$$

The sample observed queue is depicted in Figure 3 with sample recorded frame depicted in figure 1. The crossing is illustrated in Figure 2, while Table 1 shows sample observations.

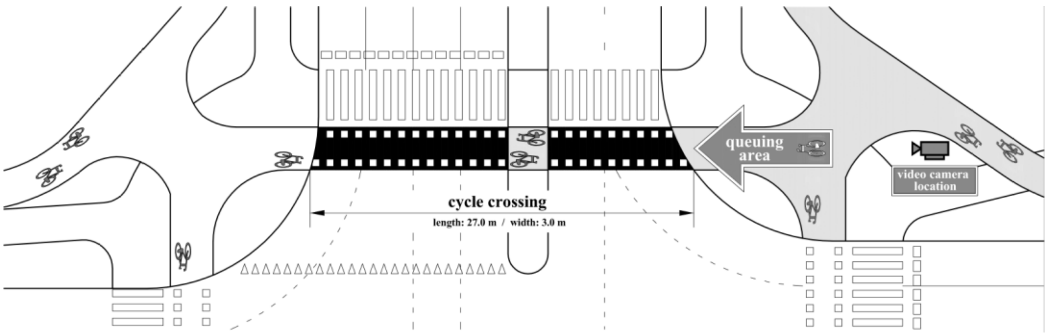


*Figure 2.* *Cycleway crossing analysed in the paper*

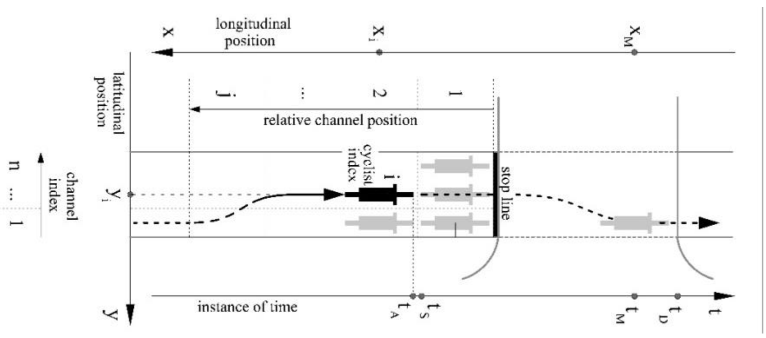


*Figure 3.* *Sample queue (Q(5,3)) representation*

**Table 1. Sample observations**

| queue index | cyclist index $i$ | channel index $n$ | channel position $j$ | $t_a$ [s] | $x_a$ [m] | $y_a$ [m] | $t_s$ [s] | $t_d$ [s] | $x_m$ [m] | $t_m$ [s] |
|---|---|---|---|---|---|---|---|---|---|---|
| 1 | 1 | I | 1 | -27.4 | 0.5 | 0.7 | 0.7 | 8.5 | 0.5 | 0.7 |
| | 2 | I | 2 | -25.1 | 2.5 | 0.6 | 1.8 | 9.9 | 2.5 | 1.8 |
| 2 | 1 | I | 1 | -18.0 | 0.5 | 0.5 | 0.3 | 8.0 | 0.5 | 0.3 |
| | 2 | I | 2 | -14.8 | 2.5 | 0.8 | 1.0 | 10.8 | 2.5 | 1.0 |
| | 3 | II | 1 | -15.5 | 0.5 | 1.7 | 0.5 | 9.2 | -12.0 | 6.0 |
| 3 | 1 | I | 1 | -23.3 | 0.5 | 0.8 | 0.9 | 10.4 | 0.5 | 0.9 |
| | 2 | II | 1 | -1.5 | 1.0 | 2.0 | 1.7 | 10.8 | -7.0 | 6.7 |

### 3.3 *Data analysis*

The above presented formalization allows to analyse the data and describe the multichannel behaviour. The ultimate picture resulting from the analysis can be visualised with the following queue space-time diagram (Figure 4), i.e. set of trajectories of each queueing cyclist $x_i(\tau)$ reconstructed from points and times identified in eq. 7.

The x-axis on fig.4 denotes time τ with zero being the instance when signal turns green. The y-axis denotes distance $x$ from stop line and the plots are cyclists' trajectories. Each cyclist is represented with his trajectory $x_i(\tau)$ fixed at specific points of: enqueueing at time $t_a$ at position $x_a$, starting (driving off) from the same (spatial) position at time $t_s$ (marked with circle), and discharging at time $t_d$ (marked with diamond). To depict the multichannel behaviour, we use different line styles for marking the channels.

The space-plot diagram allows to visually investigate key properties such as: number of channels; channels' formation process; channel and queue lengths; starting process and discharge times; enqueueing, starting and discharging sequences and violations among them - for which we define further our analytical approach below.

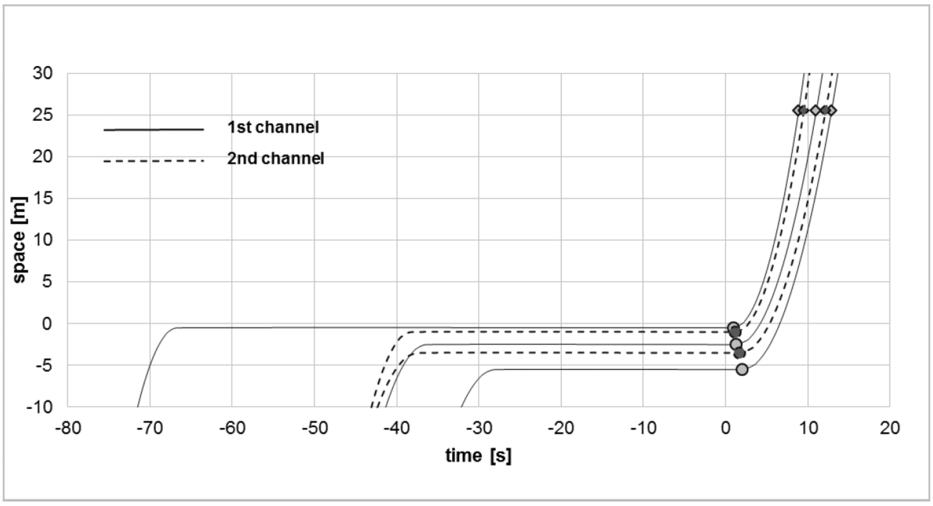


*Figure 4. Space-time diagrams of cyclists in the Q(5,2) multichannel queue*

#### *Number of channels*

The proposed formalization allows to identify number of channels in the queue and thus track the relation between queue size and number of channels. Analogously to motorised traffic, we presume that the right channel will be chosen by default and the channels to the left will be created later. Consequently, for short queues we would mainly observe single-channel formations, whereas second and third channels will be created once the first one exceeds a certain length. Notably, the formation process is non-deterministic (as cyclists are free to choose their channel), so the queue of a given length can be composed of a various number of channels. To quantify this, we analyse the number of channels $N$ as a function of queue size:

$$N(Q) = f(\|Q\|) \tag{8}$$

Such analysis allows to understand the expected number of channels formed for a given queue size along with its variability.

*Queue formation process*

To complement the above, we analyse the queue formation process by looking at the order in which arriving cyclists enqueue into the respective channels. They make the decision to enqueue into specific channel by observing the queue formation at the time of their arrival. They are not aware of the future queue evolution and only observe the results of preceding cyclists' decisions. We try to understand the main factor driving the resulting enqueueing decision. Our hypothesis is that this could be motivated by the expected time savings to be gained from enqueueing into the shorter channel.

Below we introduce the generic multinomial logit formulation of such choice model, where the probability $p$ of selecting the channel $a$ at the arrival into a queue of a given structure (channel lengths $\{a|b|c\}$) is calculated from the channel utilities, expressed as a function of channel length multiplied by negative $\beta$'s and adjusted with constant $ASC$ (in order to "skew" the choice towards the right-side channels, reflecting the natural tendency of right-hand side traffic):

$$p(a|\{a|b|c\}) = \frac{\exp(\beta \cdot a + ASC_a)}{\exp(\beta \cdot a + ASC_a) + \exp(\beta \cdot b + ASC_b) + \exp(\beta \cdot c + ASC_c)} \tag{9}$$

The proposed method can be used to estimate discrete choice model and verify the above hypotheses on MNL structure and utility formulations. Such model would allow to simulate sequentially the queue formation process and further describe its probabilistic properties.

*Queue and channel length*

Length[4] of the multichannel queue can be analysed in a twofold manner: first with respect to the channel lengths, and then with respect to the resultant queue length. Queue/channel length is readable from the space-time diagram (Figure 4) as the distance of the last cyclist from the stop line (y-axis). Whereas for car traffic stopping in regular lanes, the queue length can be approximated from average vehicle length plus the average gap multiplied by the channel size, this seems more complex for the bicycle traffic. As we observed in field, cyclists tend to stop close right behind each other, and overlap within the channel, thereby standing ('packing') more densely within a queue. To analyse this phenomenon, we represent the channel length as a function of channel size and verify the linearity of this relation:

$$l(C) = f(\|C\|) \tag{10}$$

Queue length is, in turn, the length of the longest channel in the queue, and it thus depends on: 1) the number of formed channels and 2) the length of the longest channel. It is then directly related to the multichannel behaviour, and we do not expect the queue length to simply increase proportionally by mean bicycle length for each additional cyclist. We reckon that, due to more effective space utilization of multichannel queues, the mean space occupied per each queuing

[4] Note that now we refer to the physical channel length understood as the distance between the last (furthest) cyclists from the stop line in meters, contrary to the size, being the cardinality $\|Q\|$. The queue and channel length measures obtained with the proposed method refer to distances between the stop line and the front axis of the last queueing cyclist (see Figure 3). To obtain the actually occupied space, one shall add the mean length from bicycle front axis to the end of the rear wheel to the presented measures.

cyclist would be less than 1.6 meter (average observed value for a channel). However, this value would likely vary between long single-channel queues and short multichannel queues with evenly distributed channel lengths. To analyse queue length, we express it as a function of queue size:

$$l(Q) = f(|Q|) \tag{11}$$

*Cyclists' starting times*

When the queue is formed and the traffic signal turns green, cyclists start riding. Cyclists' starting times were analysed and defined as the duration between the instances when signal turns to green phase and when cyclist starts riding, i.e. lifts the foot from the ground. This instance can be read from the space-time plot (Figure 4) as the value on time axis when the cyclist drives off (marked with circle). We presume that the FIFO discipline will be kept within the channel, but not necessarily for the multichannel queue as a whole. Our aim was to verify whether cyclists in the channel start riding sequentially and if there is a linear correlation between starting time and their position in the channel. We presume that the starting time may be dependent primarily on the cyclist's position in the channel, but may also vary with the channel index and queue structure. Analogous to car traffic, we may expect left-hand side channels to be faster than right-hand side ones. The merging process, although apparently seamless, may either delay cyclists at the back, as they need to allow others to merge in front of them, or on the contrary - facilitate their faster reaction and thus induce decision to overtake others.

We represent the cyclist's starting time as a function of his position, channel index and start time of his predecessor in that channel and analyse the resulting relations:

$$t_s(x_i) = f(j, n, N(Q), t_s(x_{i-1})) \tag{12}$$

With such formulation we can verify if cyclists in the second and third channel react faster than the cyclists in the first one. We can also verify if there is a certain 'pressure' exerted upon the preceding cyclists, i.e. whether they tend to react quicker, being aware of other cyclists queueing behind them. It should be noted here that typically used reaction times and headways may be derived from above formula and compared values reported in other studies. However, for the multichannel merging queue the headway analysis is not straightforward and may be confusing.

*Queue discharge*

Queue discharge time is defined as duration from the instance when traffic signal turns green till the last cyclist crosses the discharge line, visible on the space-time plot (Figure 4) as the biggest x-axis value of discharging cyclist (marked with diamond). It depends not only on number of cyclists in the queue, but also on the queue formation itself. We presume that the queue discharge time will increase with number of cyclists, but at the same time it can become more efficiently discharged through multiple channels. Note that discharge time covers two processes: the crossing time itself and the additional queue-related delay (which is of specific interest for us).

For analysis purposes, we represent the queue discharge time as a function of its size, number of channels and its structure and analyse the resulting relations:

$$t_d(Q) = f(|Q|, N(Q), \{a \mid b \mid c\}) \tag{13}$$

*FIFO and its violations*

The proposed method captures the ordered sequences of: enqueueing, starting, merging and discharging processes. These will be compared for the purposes of analysing the queue dynamics and FIFO violations. In a standard, single-channel FIFO queue those sequences are identical. For multichannel queues we are interested in more detailed differences between them which should be further analysed. This can reveal e.g. the leap-frogging behaviour, i.e. if the cyclists from the first channel are overtaken by cyclists from the second and third channels as they merge. It may also support the hypothesis that second and third channels are used to leap-frog other queuing cyclists and minimize the time losses. To illustrate the phenomenon, we present selected observations of *Q(5,2)* queue in Figure 5. The third cyclist to enqueue is the leader of his channel (second channel) and starts riding as the first one, yet he is overtaken at the merging process by the fifth enqueueing cyclist who merges and ultimately discharges as the first one. The cyclist who arrived first starts second, is overtaken at the merging process and discharges as third in order. The FIFO violations are identified as intersections of two cyclists' trajectories on the plot. To analyse these violations, we compare sequences of enqueue and discharge instances by means of a following matrix representation:

$$M = (m_{ed}) \in \mathbb{N}^{s \times s} \tag{14}$$

, where $s$ is the queue size and value in cell $m_{ed}$ denotes number of cyclists arriving at $e$-th position and discharging at $d$-th position. In such representation, FIFO observations are on the diagonal, and its violations can be seen in both lower (overtaking) and upper (being overtaken) triangles.

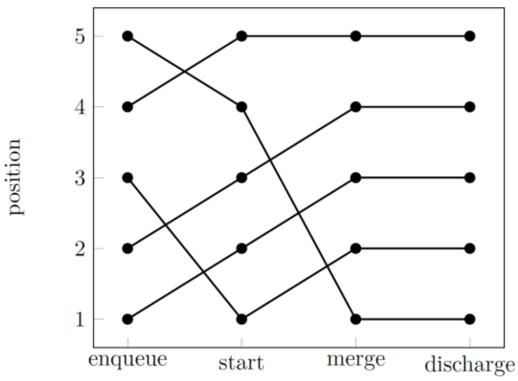


*Figure 5. Ordered sequences of the fifth cyclist in the queue Q(5,2) violating the FIFO principle (marked by points where the lines cross each other)*

## 4. Results

This chapter summarizes the field observation results and reports key findings. Results' summary follows the same order as the methodology explanation in previous chapter, starting with the number of channels formed, then extended with detailed queue formation process and enqueueing decision characteristics. Further on, we report the observed channel lengths and resulting queue lengths. These are followed by the description of cyclists' starting times within the channel and resulting queue discharge times. Next, we report on the queue discipline and demonstrate that the FIFO rule is violated for multichannel queues. To illustrate the results, we present selected space-time diagrams where the multichannel phenomena are evident. The results are briefly commented in this section and a more in-depth discussion follows in the next chapter.

### *4.1 Number of channels*

We analysed the number of channels $N$ as a function of queue size $\|C\|$ (number of cyclists) in Figure 6. We reported how many channels are formed for respective queue sizes. Bars denote the relative shares and numbers denote absolute number of observations.

A crucial observation[5] is that the share of observed single-channel queues negatively correlates with queue size. If two cyclists are queuing only, they are likely to stand one behind another in a single channel (70% of observed *Q(2,n)* queues were of type *Q(2,1)*). In that case, the share of single-channel queues drops to 50% for three-cyclist queues ($i$ = 3) and to merely 10% for more than three cyclists in the queue ($i$ > 3). Conversely, two-channel queues are observed for 30% of *Q(2,n)* queues, 50% of *Q(3,n)* queues and 70% of *Q(4,n)* queues. For $i \geq 4$ the third channel starts to be formed. The three-channel queues are observed for 20% of *Q(4,n)* queues and 44% of *Q(5,n)*. No queues of six cyclists were reported during our observations and the single observed queue of seven cyclists was formed in three channels.

For the collected sample, the average number of channels correlated positively with number of cyclists and steadily increased from 1.3 for $n$ = 2, to 2.33 for $n$ = 5. Yet, at the same time, the results reveal that the queue formation process is fairly non-deterministic. For instance, four cyclists can form a *Q(4,1), Q(4,2)* or *Q(4,3)* queue which has important implications for length and discharge time as we will show below.

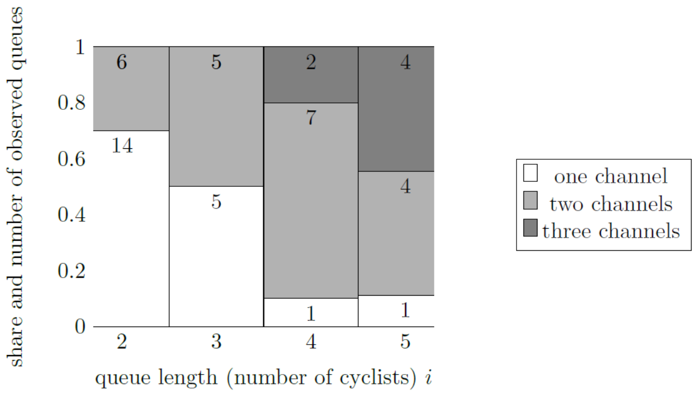


*Figure 6.* *Number of channels in observed queues*

## *4.2 Queue formation*

Table 2 presents how the *Q(4,n,{a|b|c})* queues were formed[6]. When we observed two channels (7 out of 10 such queues), this was due to one of the cyclists deciding to enqueue into the second channel. In most cases (4 out of 7), the first three cyclists enqueue into the first channel and the fourth arriving cyclist stops next to them in a second channel. The cases in which second or third cyclist already forms a new channel were also observed, but less frequently. Four cyclists formed three channels only twice during our observations. Interestingly, we observed a queue where first three cyclists already formed three parallel channels, which may be attributed to them already travelling together in a group. Table 3 depicts the same situation for *Q(5,n,{a|b|c})* queues. Here, somehow contrary to *Q(4,n,{a|b|c})* queues, the second cyclist already decided to enqueue into a second channel (for 5 out of 9 observed queues). To resolve this, we focus further on enqueueing decisions below.

[5] For brevity we use *Q(i,n)* to denote the queue of $i$ cyclists who formed $n$ channels.
[6] Here we extend the queue notation from *Q(i,n)* to *Q(i,n,{a|b|c})* to denote the number of cyclists in the first (a), second (b) and third (c) channel respectively.

**Table 2. Formation process of *Q (4,n)* queues**

| queue type | Q (4,1, {4\|0\|0}) | | | Q (4,2, {3\|1\|0}) | | Q (4,2, {3\|1\|0}) | | Q (4,2, {3\|1\|0}) | | Q (4,2, {3\|1\|0}) | | Q (4,3, {2\|1\|1}) | | | Q (4,3, {2\|1\|1}) | | |
|---|---|---|---|---|---|---|---|---|---|---|---|---|---|---|---|---|---|
| no. of observations | 1 | | | 4 | | 1 | | 1 | | 1 | | 1 | | | 1 | | |
| channel *n* | I | | | I | II | I | II | I | II | I | II | I | II | III | I | II | III |
| arrival index *i* | 1 | | | 1 | 4 | 1 | 3 | 1 | 2 | 2 | 1 | 1 | 4 | 3 | 1 | 2 | 3 |
| | 2 | | | 2 | | 2 | | 3 | | 3 | | 2 | | | 4 | | |
| | 3 | | | 3 | | 4 | | 4 | | 4 | | | | | | | |
| | 4 | | | | | | | | | | | | | | | | |

**Table 3. Formation process of *Q (5,n)* queues**

| queue type | Q (5,1, {5\|0\|0}) | Q (5,2, {3\|2\|0}) | | Q (5,2, {3\|2\|0}) | | Q (5,2, {3\|2\|0}) | | Q (5,3, {3\|1\|1}) | | | Q (5,3, {3\|1\|1}) | | | Q (5,3, {3\|1\|1}) | | |
|---|---|---|---|---|---|---|---|---|---|---|---|---|---|---|---|---|
| no. of observations | 1 | 2 | | 1 | | 1 | | 2 | | | 1 | | | 1 | | |
| channel *n* | I | I | II | I | II | I | II | I | II | III | I | II | III | I | II | III |
| arrival index *i* | 1 | 1 | 2 | 1 | 3 | 1 | 2 | 1 | 2 | 3 | 1 | 3 | 4 | 1 | 3 | 5 |
| | 2 | 4 | 3 | 2 | 5 | 3 | 4 | 4 | | | 2 | | | 2 | | |
| | 3 | 5 | | 4 | | 5 | | 5 | | | 5 | | | 4 | | |
| | 4 | | | | | | | | | | | | | | | |
| | 5 | | | | | | | | | | | | | | | |

### 4.3 *Channel enqueueing decisions*

In Table 4 we report the enqueueing decisions subject to queue composition at the arrival. We see that 88% of observed cyclists enqueue to the first channel if they arrive second, yet this figure drops to 66% if cyclists arrive third and to 13% when they arrive fourth. A general diagonal trend can be found in table 4 but it is not statistically strong. An interesting finding is that 13 out of 15 cyclists arriving to *Q(3,1)* queue decide to form the second channel, forming a *Q(4,2)* queue. None of the subsequent cyclists arriving to such formed *Q(4,2,{3|1|0})* queue decides to enqueue to the first channel. This supports the hypothesis that the second channel is formed when the first one becomes too long and next arriving cyclists are likely to stop significantly closer to the stop line.

The MNL logit model (eq. 9), parametrized with $\beta = -0.4$ and alternative specific constants of 0,-2,-3 respectively, yielded MSE of 1.3 and almost 100 out of 150 enqueueing decisions were predicted correctly (note that, due to limited sample size, this should be treated as a proof-of-concept verification only rather than the proper model estimation).

**Table 4. Enqueue decisions subject to queue composition at the arrival**

| queue composition at the arrival | | {0\|0\|0} | {1\|0\|0} | {2\|0\|0} | {2\|1\|0} | {2\|2\|0} | {3\|0\|0} | {3\|1\|0} | {3\|2\|0} | {3\|2\|1} | {4\|0\|0} |
|---|---|---|---|---|---|---|---|---|---|---|---|
| enqueue | I | 50 | 44 | 20 | 0 | 0 | 2 | 0 | 0 | 0 | 1 |
| decision | II | 0 | 6 | 10 | 3 | 2 | 13 | 3 | 0 | 0 | 0 |
| (channel) | III | 0 | 0 | 0 | 2 | 1 | 0 | 3 | 1 | 1 | 0 |

### 4.4 *Channel length*

Figure 7 presents channel length as a function of the number of cyclists in the channel (i.e. channel size). As expected, subsequent cyclists in the channel stop further from the stop line. The linear estimate yields the front axis position of the first cyclist equal to 0.74m, and 1.6m for each following cyclist (compared to 1.34m reported by (Raksuntorn & Khan, 2003)). It seems that cyclists tend to queue more densely when channels are longer, further reducing the distances between them. While first cyclists in the queue may stop in a rather loose manner, i.e. usually in a single channel, cyclists approaching longer queues behave differently and either form another channel or stop closer to the preceding cyclist. This can explain the non-linearity visible in Figure 7.

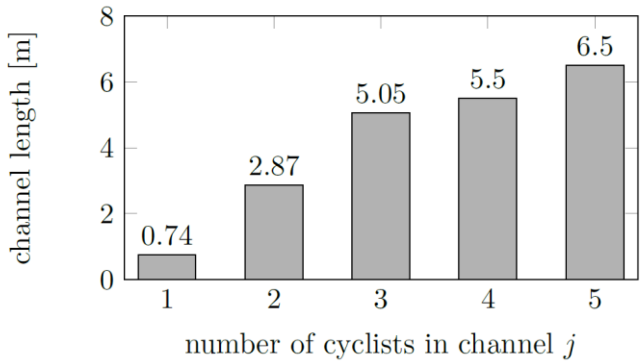


*Figure 7. Channel length vs. number of cyclists (channel size)*

### *4.5 Queue length*

We summarized the observed queue lengths with table 5 and figure 8. As expected, the average queue length increases with the total number of cyclists, analogous to the channel length. However, the average length per cyclist is around 1.1 meter, which is a significant reduction compared to 1.6 meter (per cyclist) for the channel. Furthermore, substantial variability of queue length can be observed, for instance the observed length of a *Q(3,n)* queue varied from 1.5 to 6 meters.

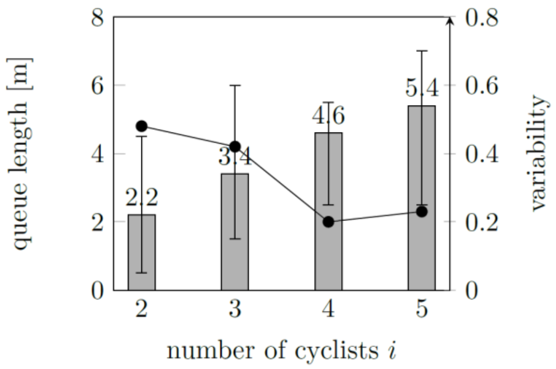


*Figure 8. Queue length vs. queue size (number of cyclists). Bars denote mean length; limits denote min and max values; line denotes the variability*

**Table 5. Queue lengths**

| number of cyclists *i* | | 2 | 3 | 4 | 5 | 7 | total |
|---|---|---|---|---|---|---|---|
| queue length [m] | average | 2.2 | 3.4 | 4.6 | 5.4 | 5.5 | 3.6 |
| | variability (std/mean) | 48% | 42% | 20% | 23% | - | 48% |
| | min | 0.5 | 1.5 | 2.5 | 2.5 | - | 0.5 |
| | max | 4.5 | 6.0 | 5.5 | 7.0 | - | 7.0 |
| mean length per cyclist | | 1.12 | 1.12 | 1.14 | 1.09 | 0.79 | 1.11 |

### 4.6 *Cyclists' starting times*

Cyclists start riding one after another and subsequent starting times are strictly increasing. The first finding is that the average observed starting time of the first cyclist in a channel decreases as the number of cyclists behind increases. We observed average values of 1.0s and 1.1s for channels of two and three cyclists, against 0.8s and 0.9s for channels of four and five cyclists (mind that such hypotheses derived from a limited pilot sample are not significantly strong). This might be attributed to a sort of additional pressure felt by first cyclist when more cyclists wait behind (see Liang et al., 2012) and further reinforced by competitive behaviour between channels. Cyclists within one channel react to the green signal onset sequentially, starting on average 0.6s after the preceding cyclist in the channel. However, the observed starting times are highly variable, for instance we could observe that the second cyclist would react in 1.7 second, the fourth in 1.8 seconds - but the fifth would only react after almost five seconds. Those variations are also reported by (Raksuntorn & Khan, 2003) where reaction time of the first cyclist varied from 0.2 to over 5 seconds, decreasing asymptotically to an average of 0.8s - which compares with our findings.

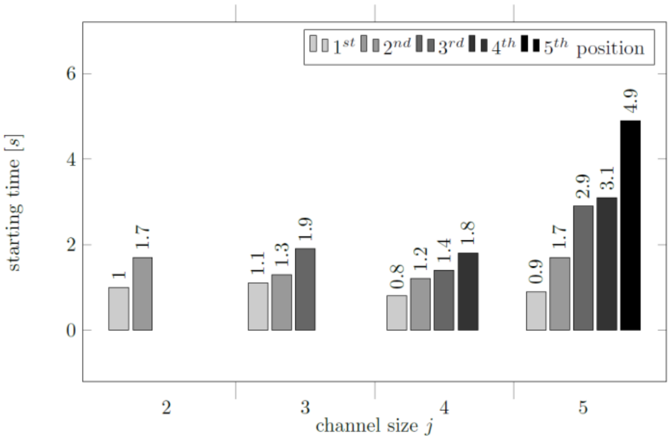


*Figure 9. Starting times of consecutive cyclists in channel for various channel sizes*

The starting time of the first cyclist depends also on number of channels, being apparently shorter for multichannel queues (Figure 10). Interestingly, in such queues it is the cyclist from the first channel (rightmost) who will usually react first. Seemingly, this could be induced by the feeling of being challenged by cyclists on his left side. Consequently, the starting time of the first cyclist drops from an average of 1.5s for single-channel queues to below 1.0s for multichannel queues. Also, it seems that cyclists in the first channel (on the right side) react faster (start time of ca. 0.9s) than cyclists in second and third channels (ca. 1.2s). Again, we stress that those results are obtained on a small, pilot sample, and our objective here is only to reveal the phenomena without deriving strongly supported descriptions. Nonetheless, we hypothesize that the reason for this behaviour may be that cyclists on the right side might somehow try to prevent from being overtaken, and thus aim to remain at the earlier positions (i.e. at the forefront of discharging queue) as much as possible.

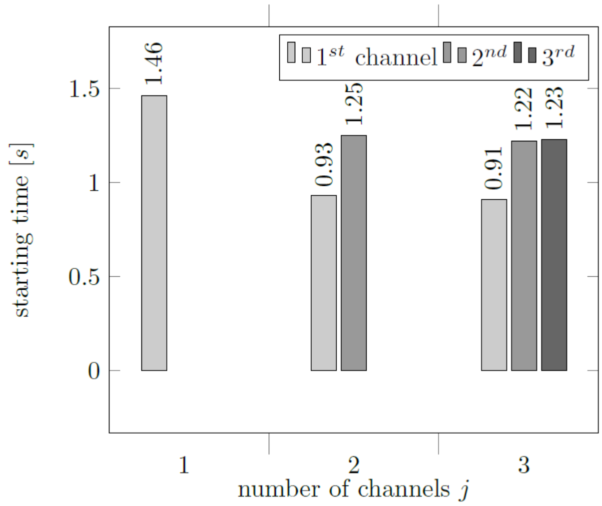


*Figure 10.* *Starting times of the first cyclist in a channel for various queue configurations*

### *4.7 Queue discharge time*

Queue discharge times are shown in Figure 11 in two dimensions: i.e. with reference to the total queue size and to the number of channels. Although the queue discharge times rises with number of cyclists, this trend does not seem to be significant. It is clearly visible though that discharge times are substantially shorter for multichannel queues. For instance, discharging time of a *Q(5,1)* queue is equal to 16s, while discharging time of a *Q(5,3)* queue equals 12s (of which the crossing time itself takes around 9s). Moreover, the *Q(5,1)* queue discharges longer (16s) than a multichannel, seven-cyclist queue (13s).

The central finding is that the total queue discharge time strongly depends on the number of channels: multiple channels reduce the queue discharge time by ca. 5s for the observed queues of five cyclists. Again, it should be noted that discharge time is non-deterministic, since the number of channels is non-deterministic itself (see Figure 6). Notably, multichannel queues can strongly reduce the green signal time needed to discharge the queue and thus optimize the signal performance.

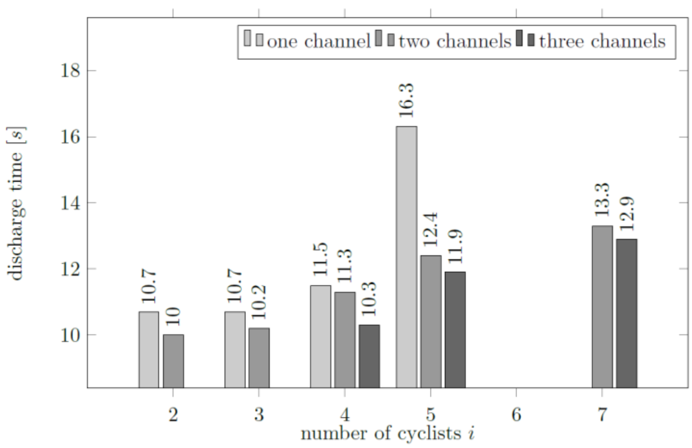


*Figure 11.* *Queue discharge times for various number of cyclists and queue configurations*

Additionally, we plot the enqueueing positions $x_a$ against discharge time $t_d$ in figure 12, where we distinguish between cyclists in various channels. The strong variance in the first position can be somehow traced on a diagonal trend, though this becomes less evident for second and third channels. Surprisingly, some of cyclists in the first channel discharge at quick pace despite their further stop position, which suggests that overtaking occurs also within a channel.

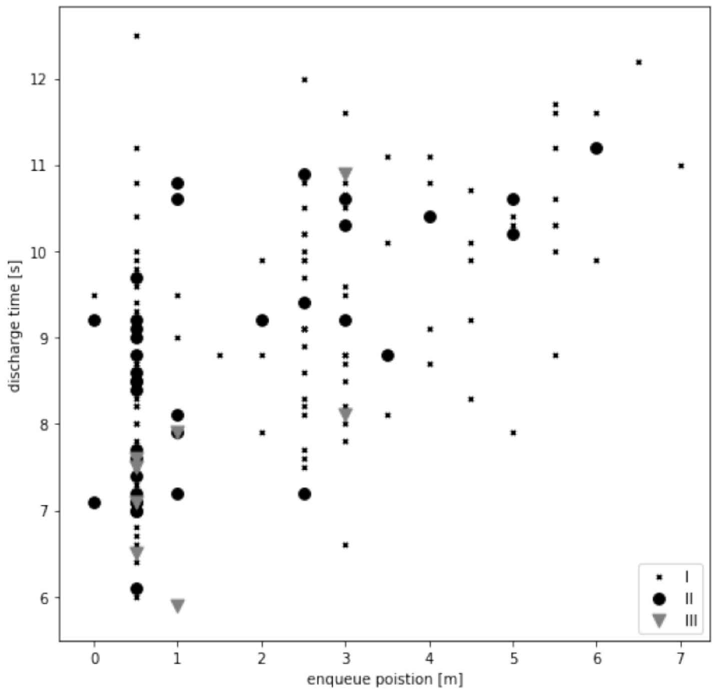


*Figure 12. Enqueueing position vs. discharge time in respective channels*

*4.8 Overtaking and leap-frogging behaviour*

It could be expected that one of the reasons behind formation of additional (second and third) channels would be the willingness of arriving cyclists to overtake ('leap-frog') those already waiting in the first channel. This can be already supported with the findings from the enqueueing decision process (see Table 4), yet it also somehow contradicts the findings regarding starting (drive-off) times (see Figure 9).

To gain further insight into these phenomena, we illustrate the observed FIFO violations with a matrix $M$ (eq. 13), where the enqueueing order index (row) is shown against the discharging order index (column). We depict these separately for cyclists queueing in the first channel (Table 6) and for those in the second and third channels (Table 7).

It can be seen that the enqueueing order can strongly deviate from the discharging order. For instance, we observed cyclists arriving first and discharging fourth in order, as well as cyclists arriving sixth and discharging first. Aggregated results in Table 6 show that 49% of cyclists in the first channel discharged from a later (further) position that they arrived, 26% kept the same position (index) and 25% evacuated from an earlier position. Results in Table 6 show that just a single observed cyclist from the second or third channel discharged from a later position than the one they have arrived at, roughly 25% kept the position constant (obeying the FIFO rule), and almost 75% evacuate from an earlier position overtaking other cyclist(s). This supports the hypothesis that second and third channels are often used to leap-frog other queuing cyclists and minimize the time losses.

**Table 6. Arrival vs. discharge index for cyclists in the first channel**

| | | discharge index | | | | | | |
|---|---|---|---|---|---|---|---|---|
| | | 1st | 2nd | 3rd | 4th | 5th | 6th | 7th |
| arrival index | 1st | **15** | 12 | 2 | 2 | 0 | 0 | 0 |
| | 2nd | 2 | **4** | 13 | 4 | 1 | 1 | 0 |
| | 3rd | 0 | 0 | **1** | 8 | 3 | 0 | 1 |
| | 4th | 4 | 8 | 3 | **2** | 1 | 0 | 0 |
| | 5th | 1 | 1 | 1 | 3 | **3** | 0 | 0 |
| | 6th | 1 | 0 | 0 | 0 | 0 | **0** | 0 |
| | 7th | 0 | 0 | 0 | 0 | 0 | 0 | **0** |

**Table 7. Arrival vs. discharge index for cyclists in the second and third channel**

| | | discharge index | | | | | | |
|---|---|---|---|---|---|---|---|---|
| | | 1st | 2nd | 3rd | 4th | 5th | 6th | 7th |
| arrival index | 1st | **0** | 0 | 0 | 0 | 0 | 0 | 0 |
| | 2nd | 2 | **4** | 0 | 0 | 0 | 0 | 0 |
| | 3rd | 6 | 2 | **2** | 0 | 0 | 0 | 0 |
| | 4th | 4 | 8 | 3 | **2** | 1 | 0 | 0 |
| | 5th | 1 | 1 | 1 | 3 | **3** | 0 | 0 |
| | 6th | 1 | 0 | 0 | 0 | 0 | **0** | 0 |
| | 7th | 0 | 0 | 1 | 0 | 0 | 0 | **0** |

### *4.9 Space-time trajectories*

We synthesise the above analysis by plotting the queue $Q$ space-time diagrams $x_i(\tau)$. The x-axis denotes the time $\tau$ with zero being the instance when traffic signal turns green, the y-axis denotes the distance x from stop line. Plots represent the individual cyclists' trajectories. The trajectory $x_i(\tau)$ of each cyclist is fixed at specific reference points, which are: enqueueing time instance ta at position $x_a$, starting time instance (from the same spatial position) $t_s$ (marked with circle), and discharging time instance $t_d$ (marked with diamond). To better illustrate the multichannel queuing behaviour, we distinguished channels with specific line styles. We assumed typical and generic assumptions regarding the acceleration and deceleration profiles of cyclists, solely for illustrative purposes.

To demonstrate our results, we present below space-time diagrams for a five-cyclist queue in case they would form a single channel (Figure 13), two channels (Figure 14) and three channels (Figure 15). The differences between them clearly indicate how formation of multiple channels contributes towards reductions both in the queue lengths and discharging times.

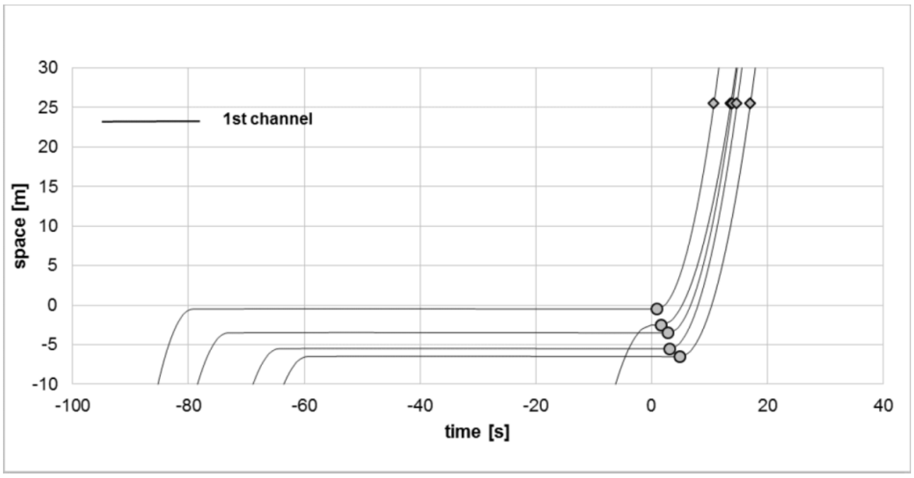


*Figure 13. Space-time diagram for cyclists in the Q(5,1) single-channel queue*

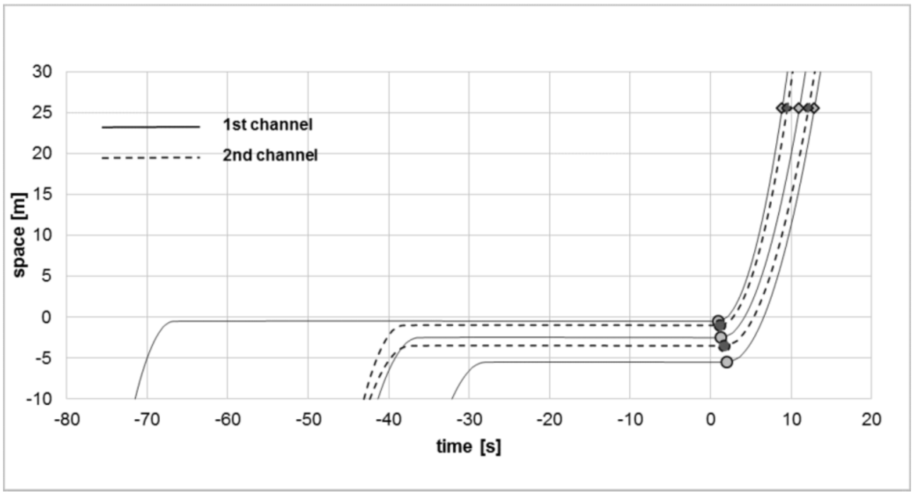


*Figure 14. Space-time diagram for cyclists in the Q(5,2) multichannel queue*

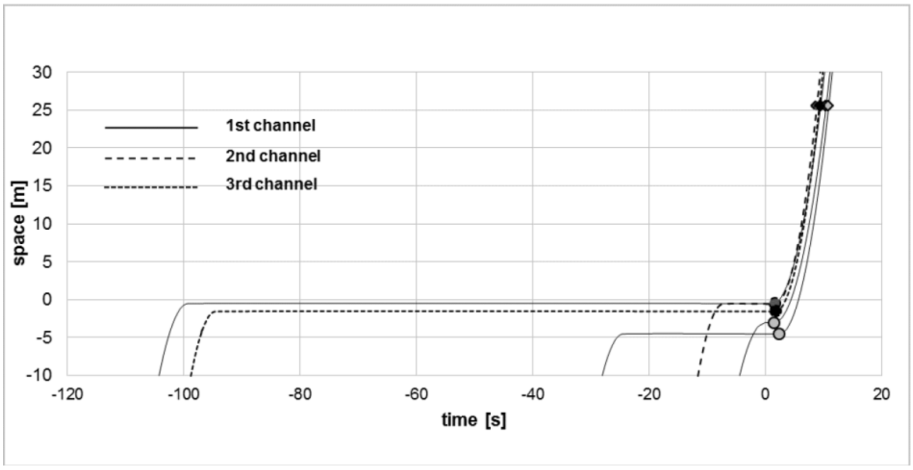


*Figure 15. Space-time diagram for cyclists in the Q(5,3) multichannel queue*

# 5. Conclusions

The objective of this study was to propose and demonstrate a complete method to analyse the bicycle queuing behaviour at signalized cycle crossings. The method focuses on specific property of bicycle traffic flow, i.e. multichannel queuing phenomena, which seem not to have been thouroughly investigated in state-of-the-art research. In this work, we present the proposed methodology and then apply it to our case study observations of cyclist queues, in order to understand their queuing behaviour and the associated phenomena. Field observations were conducted for a signalized cycle crossing in the city of Krakow (Poland), where we video-recorded a pilot sample of ca. 50 cyclist queues. We report results for our case study and demonstrate how the introduced method can enhance the analysis of cyclist queuing behaviour.

Findings indicate that the multichannel queue formation and discharging process might significantly impact the efficiency of bicycle queues at signalized crossings. Cyclists at intersections tend to form multichannel queues which are shorter in length and discharge at faster rate than a single-channel queue. This is a beneficial phenomenon both for individual cyclists who might gain in terms of time savings by enqueueing into additional (second, third etc.) channels, and at an aggregate level - i.e. for the queue as whole, as it contributes to improved space utilization and discharging performance. However, we observe that the multichannel queuing behaviour is a highly variable and non-deterministic phenomenon, and its' performance analysis is strongly related to the queue formation process, i.e. how the arriving cyclists form consecutive queue channels. Detailed findings from the pilot study can be summarized as follows:

1. Even though the analysed cycle crossing is located along a single-lane, bidirectional cycle crossing with a constant approach width (i.e. no extra widening within the crossing), multichannel queue formation is a common occurrence. Cyclists form multiple channels and merge seamlessly as they exit the crossing, without creating conflicts with cyclists incoming from the opposite direction.
2. Number of channels is strongly correlated with the queue size and queue formation process. It was unlikely to observe a single-channel queue if there were more than 2 or 3 cyclists queuing at the crossing. Crucially, the queue formation process exhibits a fairly non-deterministic pattern: a queue of 5 cyclists could have been formed either as a two- or three-channel queue, or (less likely) a single-channel queue. Vast majority of observed cyclists started forming a second channel when they arrived fourth, i.e. once the 3 already waiting cyclists have formed the first channel. Based on the results, we hypothesize that cyclists decide to form another channel once differences between channel sizes exceed a certain (perceived) threshold length.
3. The channel length does not increase linearly with channel size (i.e. number of cyclists), but spacing between cyclists tends to decrease as cyclists at further positions are standing more densely within the channels. Total queue length is related to the number of channels, though apparently this correlation is difficult to determine more conclusively: firstly, the queue can be formed by a variable number of channels, and secondly the channel lengths themselves can vary substantially. Consequently, we observed total length of a 3-cyclist queue ranging between 1.5 - 6.0 meters, depending on the number of formed channels. Such variability is a specific feature of short cyclist queues: total queue length became less variable as the number of cyclists increased. Crucially, multichannel queuing behaviour could lead to significant improvements in space utilization: we observed an instance when 5 queuing cyclists formed a multichannel queue of only 2.5 meters in length a significant difference compared to the same, single-channel queue (6.5m).
4. Starting time of the first cyclist becomes shorter as the channel length increases (from ca. 1.1 seconds for shorter channels down to ca. 0.9 seconds for longer channels) which could be perhaps explained by a certain perception of pressure being "exerted" by a rising number of queuing cyclists. The average value was also higher for a single-channel queues (ca. 1.4 seconds) than for multichannel queues (ca. 1.0 seconds). As we observed, it was usually the cyclist in the first channel on the right that started the discharging process. In a summary, formation of multiple channels noticeably reduces total queue discharging time the discharge time of a single-channel queue of 5 cyclists was longer (16 seconds in total) than that of a multichannel queue of 7 cyclists (13 seconds), and also 5 seconds longer than discharge time of the same 5-cyclist queue but formed in multiple channels.
5. Interesting observations can be also derived from the observations of queue formation and discharging sequence. We observed 2 various queuing disciplines: while cyclists within the channel dissipate in the FIFO order, there seems to be no fixed discipline in the queue discharging order as a whole. Notably, on the aggregate level, multichannel queuing behaviour results in noticeable violations of the FIFO discipline: ca. 50% of cyclists in the first channel discharged at a further (later) sequence than they have arrived in the queue, while ca. 75% of cyclists in the second and third channels managed to "leap-frog" others. This seems to

support the hypothesis that second and third channels might be often used to overtake other queuing cyclists and minimize the time losses.

A certain limitation of our study could be attributed to the sample size obtained to illustrate the method. We measured ca. 50 measured cyclist queues of relatively short lengths (max. 7 cyclists per queue) and only at a single observation site. Despite this, we believe that the study resulted in valuable findings, and the proposed method used in further broader research in the future shall provide a much deeper insight into the examined phenomena, with statistically more solid conclusions.

The introduced methodology could be of relevant importance to research on bicycle flow modelling, as both micro- and macroscopic models for bicycle flows would benefit from findings on the multichannel queuing phenomena. Results presented in this paper further reinforce the notion that bicycle traffic should be modelled predominantly on a grid-like approach (i.e. analogous to pedestrian traffic) to account for high flexibility in both longitudinal and lateral movements rather than modelling them with a strict lane-discipline approach (as motorized traffic) which could oversimplify important phenomena. One important and still unrevealed factor seems to be cycling in groups, as cyclists riding together could enqueue in parallel channels (side-by-side) at signalized crossings. This could also explain some non-optimal behaviour (see similar findings on pedestrians by (Porzycki et al., 2014)).

Finally, findings on multichannel queuing behaviour should serve as crucial basis for practical indications, applicable among others in cycling infrastructure design guidelines. First conclusion is that extra widths should be envisaged at cycle crossing approaches (inlets), so that cyclists could form multichannel queues which are more efficient in terms of space utilization and discharge times. This leads to another conclusion, which states that both queue length and evacuation times are not necessarily a linear function of queue size (i.e. number of queuing cyclists) this apparently being the case especially for relatively shorter cyclist queues (of ca. 3-7 cyclists) which may emerge frequently and routinely at cycle crossings. In such case, reductions in waiting bay lengths and shorter green signal times could be considered. Application of the methodology demonstrated in this paper would further reinforce these notions and provide statistically sound conclusions, directly applicable in bicycle traffic engineering design and practice.

## References

Beitel, D., Stipancic, J., Manaugh, K. and Miranda-Moreno, L. (2017) Exploring Cyclist-Pedestrian Interactions in Shared Space Using Automated Video Conflict Analysis. *Proceedings of the 96th Annual Meeting of the Transportation Research Board,* Washington D.C., USA.

Botma, H. (1995). Method to determine level of service for bicycle paths and pedestrian-bicycle paths. *Transportation Research Record: Journal of the Transportation Research Board*, 1502, 38–44.

Botma, H. and Papendrecht, H. (1991). Traffic operation of bicycle traffic. *Transportation Research Record*, 1320.

Cao, J. X., Liu, R. and Li, B. (2011). Multimodal Approach to Sustained Transportation System Development: Information, Technology, Implementation. *ICTIS 2011 Proceedings*, 629–635.

Chen, P., Shen, Q. and Childress, S. (2018). A GPS data-based analysis of built environment influences on bicyclist route preferences. *International Journal of Sustainable Transportation,* 12(3), 218–231.

Deng, X. and Xu, J. (2014). Study on bicycle flow characteristics at intersections. *Civil Engineering and Urban Planning* III, 393.

Dozza, M., Piccinini, G. F. B. and Werneke, J. (2016). Using naturalistic data to assess e-cyclist behavior. *Transportation Research Part F: Traffic Psychology and Behaviour*, 41, 217–226.

Faghih-Imani, A., Eluru, N. and Paleti, R. (2017). How bicycling sharing system usage is affected by land use and urban form: analysis from system and user perspectives. *European Journal of Transport and Infrastructure Research*, 17 (3).

Figliozzi, M., Wheeler, N. and Monsere, C. M. (2013). Methodology for estimating bicyclist acceleration and speed distributions at intersections. *Transportation Research Record*, 2387, 66–75.

Ghanayim, M. and Bekhor, S. (2018). Modelling bicycle route choice using data from a GPS-assisted household survey. *European Journal of Transport and Infrastructure Research*, 18(2), 158–171.

Gon˜i-Ros, B., Yuan, Y., Daamen, W. and Hoogendoorn, S. P. (2018). Empirical analysis of the macroscopic characteristics of bicycle flow during the queue discharge process at a signalized intersection. *Transportation Research Record*, 2672(36), 51-62.

Gould, G. and Karner, A. (2009). Modeling Bicycle Facility Operation: A Cellular Automaton Approach. *Transportation Research Record: Journal of the Transportation Research Board*, 2140, 157–164.

Haifeng, J., Tao, W., Pengpeng, J. and Hun, H. (2013). Research on cyclists microscopic behaviour models at signalized intersection. *In 16th International Conference Road Safety on Four Continents*. Beijing, China (RS4C 2013). 15-17 May 2013..

Halldórsdóttir, K., Rieser-Schussler, N., Axhausen, K.W., Nielsen, O.A. and Prato, C.G. (2014). Efficiency of choice set generation methods for bicycle routes. *European Journal of Transport and Infrastructure Research*, 14(4), 332-348.

Lachapelle, U. and Cloutier, M.-S. (2017). On the complexity of finishing a crossing on time: Elderly pedestrians, timing and cycling infrastructure. *Transportation Research Part A: Policy and Practice*, 96, 54–63.

Li, Z., Li, Z., Huang, R., Yang, Z. and Ye, M. (2014). Operational Features in Bicycle Traffic Flow: An Observational Study. *Proceedings of the 94th Annual Meeting of Transportation Research Board,* Washington D.C., USA, 23.

Liang, X., Baohua, M. and Qi, X. (2012). Psychological-physical force model for bicycle dynamics. *Journal of Transportation Systems Engineering and Information Technology*, 12, 91–97.

Ling, H. and Wu, J. (2004). A study on cyclist behavior at signalized intersections. *IEEE Transactions on Intelligent Transportation Systems,* 5, 293–299.

Ma, X. and Luo, D. (2016). Modeling cyclist acceleration process for bicycle traffic simulation using naturalistic data. *Transportation Research Part F: Traffic Psychology and Behaviour,* 40, 130–144.

Miller, R. E. and Ramey, M. (1975). *Width requirements for bikeways: a level of service approach.* University of California, Civil Engineering Department.

Minge, E., Falero, C., Lindsey, G., Petesch, M. and Vorvick, T. (2017). Bicycle and Pedestrian Data Collection Manual.

Nagel, K. and Schreckenberg, M. (1992). A cellular automaton model for freeway traffic. *Journal De Physique I,* 2, 2221–2229.

Navin, F. P. (1994). Bicycle traffic flow characteristics: experimental results and comparisons. *ITE Journal,* 64, 31–37.

Nosal, K. (2015). Travel demand management in the context of promoting bike trips, an overview of solutions implemented in Cracow. *Transport Problems*, 10, 23–34.

Osowski, C. J. (2017). *Developing data collection methods to inform the quantitative design of cycle infrastructure.* PhD Thesis, University of Southampton.

Parkin, J. and Rotheram, J. (2010). Design speeds and acceleration characteristics of bicycle traffic for use in planning, design and appraisal. *Transport Policy*, 17, 335–341.

Pojani, D., Bakija, D., Shkreli, E., Corcoran, J. and Mateo-Babiano, I. (2017). Do Northwestern and Southeastern Europe Share a Common" Cycling Mindset"? Comparative Analysis of Beliefs toward

Cycling in the Netherlands and the Balkans. *European Journal of Transport and Infrastructure Research*, 17(1).

Portilla, C., Valencia, F., Espinosa, J., Nu´n˜ez, A. and De Schutter, B. (2016). Model-based predictive control for bicycling in urban intersections. *Transportation Research Part C: Emerging Technologies*, 70, 27–41.

Porzycki, J., Mycek, M., Lubas, R. and Was, J. (2014). Pedestrian spatial self-organization according to its nearest neighbor position. *Transportation Research Procedia*, 2, 201–206.

Raksuntorn, W. and Khan, S. (2003). Saturation flow rate, start-up lost time, and capacity for bicycles at signalized intersections. *Transportation Research Record: Journal of the Transportation Research Board,* 1852, 105–113.

Roess, R. P., Prassas, E. S. and McShane, W. R. (2011). *Traffic engineering*. Prentice Hall.

Romanillos, G., Zaltz Austwick, M., Ettema, D. and De Kruijf, J. (2016). Big data and cycling. *Transport Reviews*, 36, 114–133.

Shen, F., Wang, H. and Liu, H. (2011). A mesoscopic model for bicycle flow. *Proceedings of the 30th IEEE Chinese Control Conference,* July 22-24, 2011, Yantai, China, 5574–5577.

Taylor, D. and Davis, W. J. (1999). Review of basic research in bicycle traffic science, traffic operations, and facility design. *Transportation Research Record: Journal of the Transportation Research Board,* 1674(1), 102–110.

Treiber, M. and Kesting, A. (2013). *Traffic flow dynamics: Data, Models and Simulation*. Springer-Verlag Berlin Heidelberg.

Twaddle, H., Schendzielorz, T. and Fakler, O. (2014). Bicycles in urban areas: Review of existing methods for modeling behavior. *Transportation Research Record: Journal of the Transportation Research Board*, 2434(1), 140– 146.

Viti, F. and van Zuylen, H. (2004). Modeling queues at signalized intersections. *Transportation Research Record: Journal of the Transportation Research Board*, 1883(1), 68–77.

Wang, Y.G., Wei, G., Zhu, X. and Pei, Y.L. (2011). Capacity of bicycle platoon flow at two-phase signalized intersection: a case analysis of Xi'an city. *Promet-Traffic&Transportation*, 23(3), 177-186.

*WBR 2015 travel study - technical report.* (2016). Available (in Polish) at: http://transport.um.warszawa.pl/warszawskie-badanie-ruchu-2015/wyniki-wbr-2015.

Zangenehpour, S., Miranda-Moreno, L. F. and Saunier, N. (2015). Automated classification based on video data at intersections with heavy pedestrian and bicycle traffic: Methodology and application. *Transportation Research Part C: Emerging Technologies*, 56, 161–176.

Zangenehpour, S., Strauss, L., Miranda-Moreno, L. F. and Saunier, N. (2016). Are signalized intersections with cycle tracks safer? A case control study based on automated surrogate safety analysis using video data. *Accident Analysis and Prevention*, 86, 161–172.

Zhou, D., Xu, C., Wang, D. and Jin, S. (2015). Estimating capacity of bicycle path on urban roads in Hangzhou, China. *Proceedings of the 94th Annual Meeting of the Transportation Research Board*, Washington D.C., USA (2015).

Zhou, X. (2015). Understanding spatiotemporal patterns of biking behavior by analyzing massive bike sharing data in Chicago. *PloS one*, 10(10), p.e0137922.